Supplementary information of manuscript

Concurrent photochemical whitening and enhancement of ambient brown carbon

Qian Li[1], Dantong Liu[1*], Xiaotong Jiang[1], Ping Tian[2], Yangzhou Wu[1], Siyuan Li[1], Kang Hu[1], Quan Liu[3], Mengyu Huang[2], Ruijie Li[2], Kai Bi[2], Shaofei Kong[4], Deping Ding[2], Chenjie Yu[5]

[1]Department of Atmospheric Science, School of Earth Science, Zhejiang University, Hangzhou, 310027, China
[2]Beijing Key Laboratory of Cloud, Precipitation and Atmospheric Water Resources, Beijing Meteorological Service, Beijing, 100089, China.
[3]State Key Laboratory of Severe Weather & Key Laboratory of Atmospheric Chemistry of CMA, Chinese Academy of Meteorological Sciences, Beijing, 100081, China
[4]Department of Atmospheric Science, School of Environmental Science, China University of Geosciences, Wuhan, 430074, China
[5]Université de Paris Cité and Univ Paris Est Creteil, CNRS, LISA, Paris, France

Correspondence to: Dantong Liu (dantongliu@zju.edu.cn)

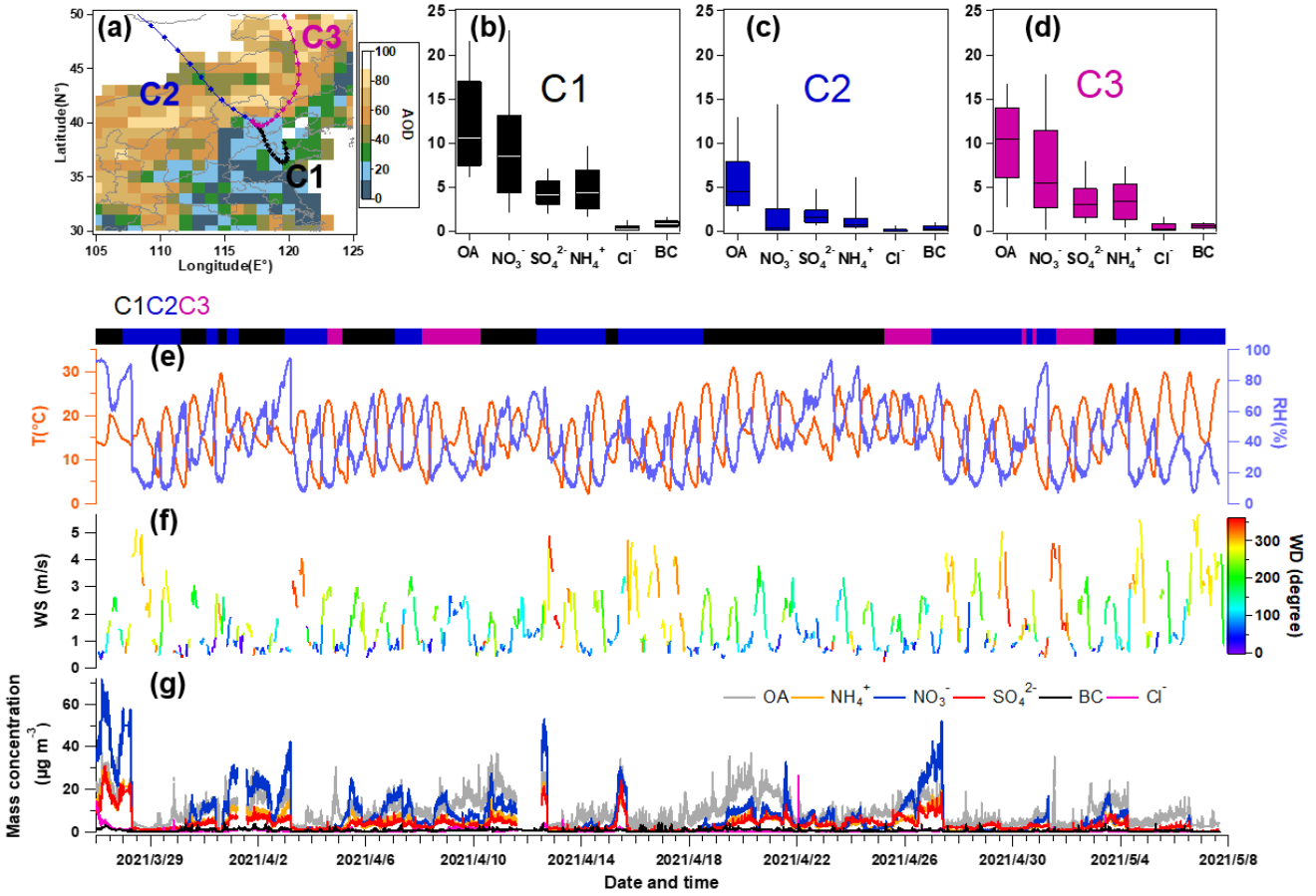

Figure S1. (a) Clustered back-trajectories for the past 72 hours during the experiment with markers denoting 12h intervals. (b-d) Statistics for the concentrations of key aerosol compositions from each cluster. The whiskers, box boundaries and lines in box denote the 10th/90th percentiles, 25th/75th percentiles and the median, respectively. (e) Time series of RH and T, (f) wind speed and colored by wind direction, (g) mass concentrations of key aerosol compositions.

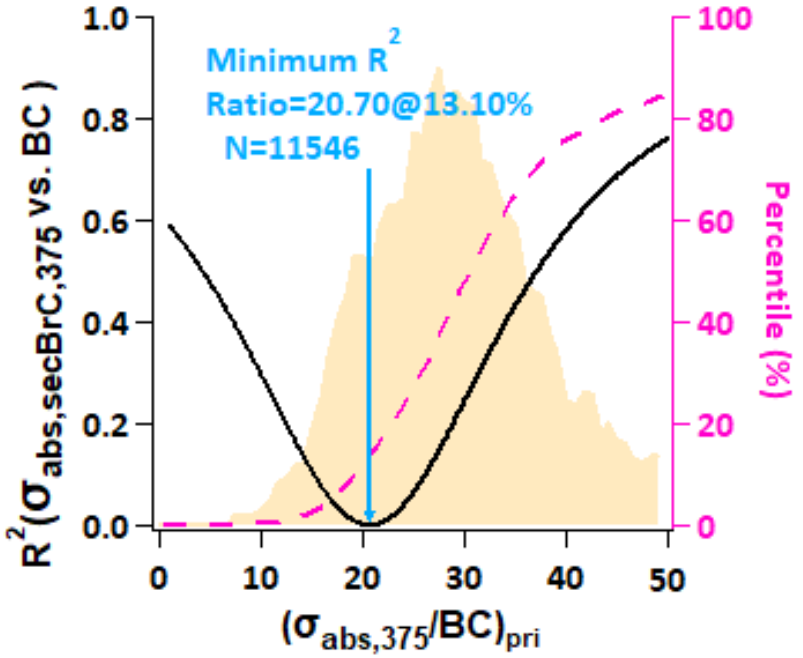

Figure S2. Minimum R-square analysis to obtain the $(\sigma_{abs,375}/BC)_{pri}$.

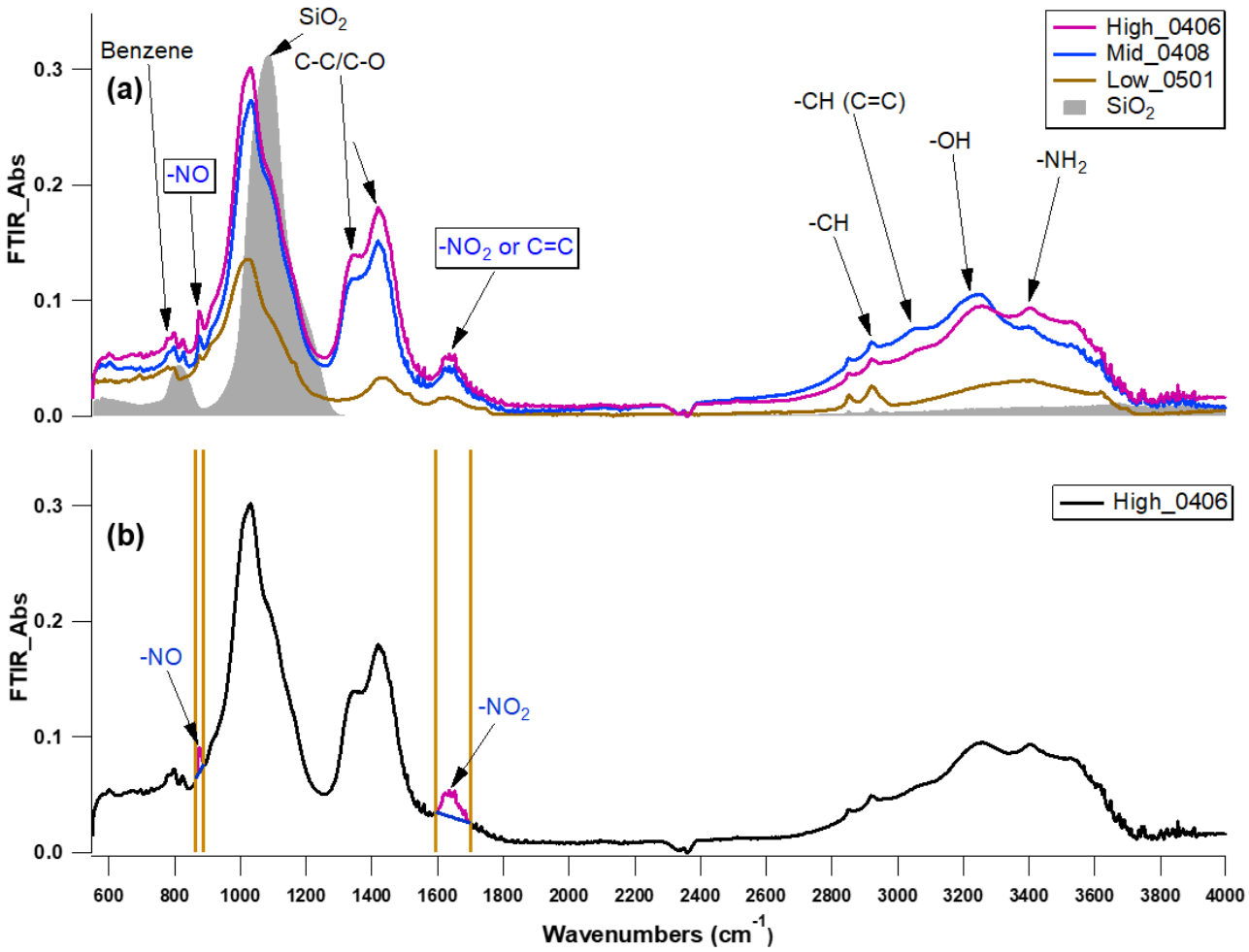

Figure S3. (a) The FTIR absorbance spectrum for the blank and filter samples during three days with different pollution levels. The main functional groups in the FTIR spectra are indicated. (b) Method of peak extraction for the -NO and -NO_2 bond.

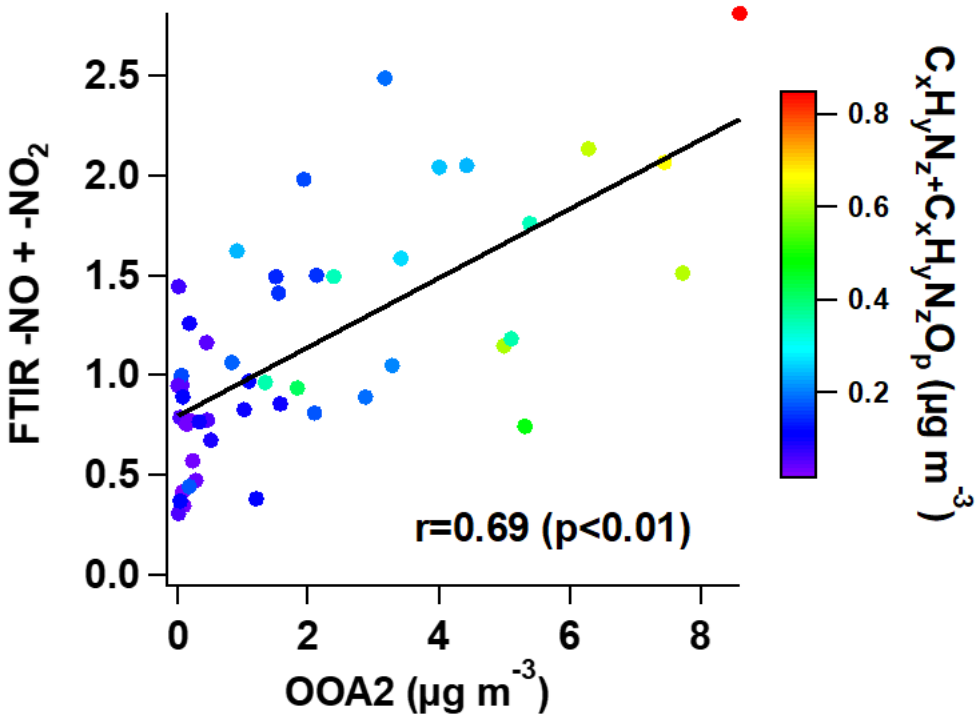

Figure S4. Relationship between the FTIR absorption of -NO, -NO_2 bond and the OOA2, colored by the $C_xH_yN_z$ and $C_xH_yN_zO_p$ fragments measured by the AMS.

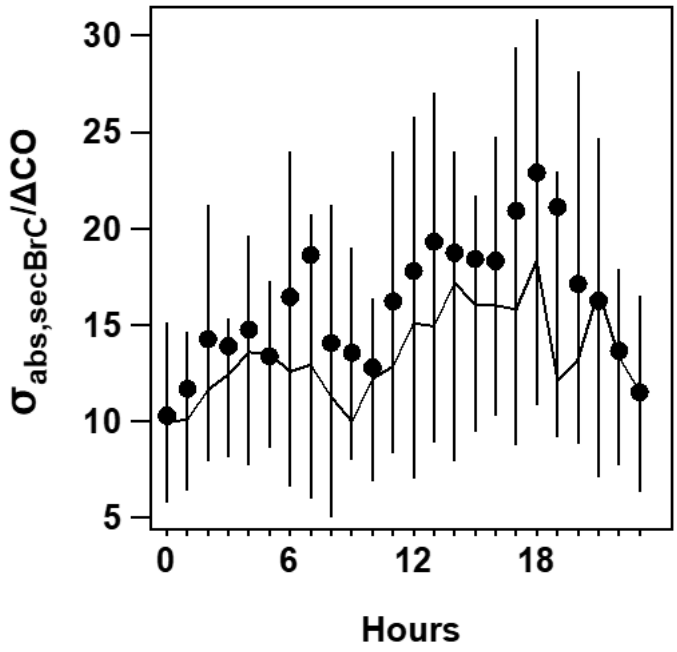

Figure S5. Diurnal variations of absorption coefficient at λ=375nm (σabs,375) for secondary BrC / ΔCO. The lines, dots and whiskers denote the median, mean and the 25th/75th percentiles at each hour respectively.

Text S1. PMF Analysis from the HR-ToF-AMS

The HR-ToF-AMS was operated in V mode with high sensitivity. High resolution mass spectra of organic matrix for m/z 12-120 were analyzed with PMF2 algorithm (Paatero and Tapper, 1994), following the data processing and factors selecting steps (Ulbrich et al., 2009; Zhang et al., 2011). The two criteria of the ratio of the scaled residuals (Q/Q_{exp}) and the rotational parameter (f_{peak}) to select the best model number of factors. The f_{peak} parameter represents the rotational sensitivity of the solution sets, and the range of the f_{peak} parameter from −1 to 1 with steps = 0.2 in our study. Factor numbers from 1 to 6 were selected to run in the PMF model.

The key diagnostic plots of 4 to 6-factor solutions are shown in Figure S5.1-3. For example, a large decrease in Q/Q_{exp} with the addition of a factor indicates that the additional factor is able to explain a significant fraction of the variation (Figure S5.1a). The presence of time-dependent structure in the residual time series suggests the need for additional factor for better fitting (Figure S5.1e). After a detailed evaluation of time series, mass spectral profiles, diurnal variations, and correlations with external tracers, the 5-factor solution with f_{peak} = 0 (Q/Q_{exp} = 2.38) was chosen.

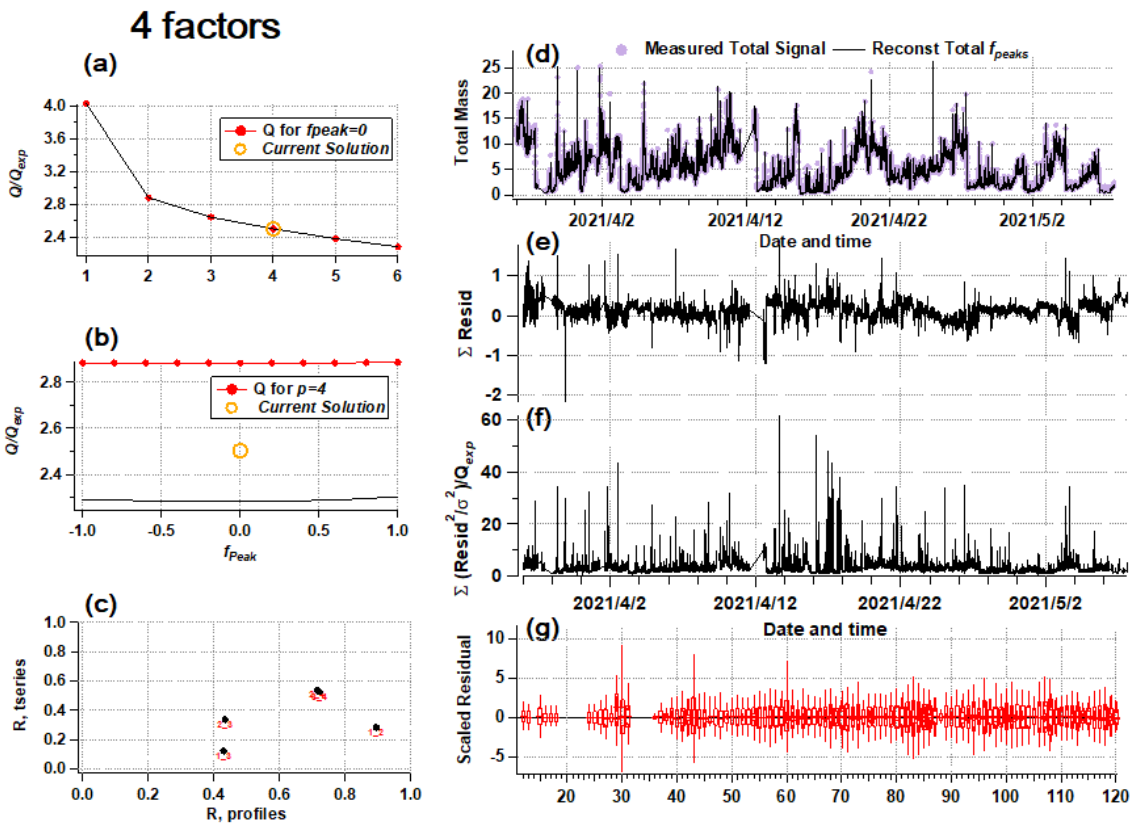

Figure S6.1 Diagnostic plots of the 4 factors of PMF analysis on OA mass spectral matrix for the spring observation.

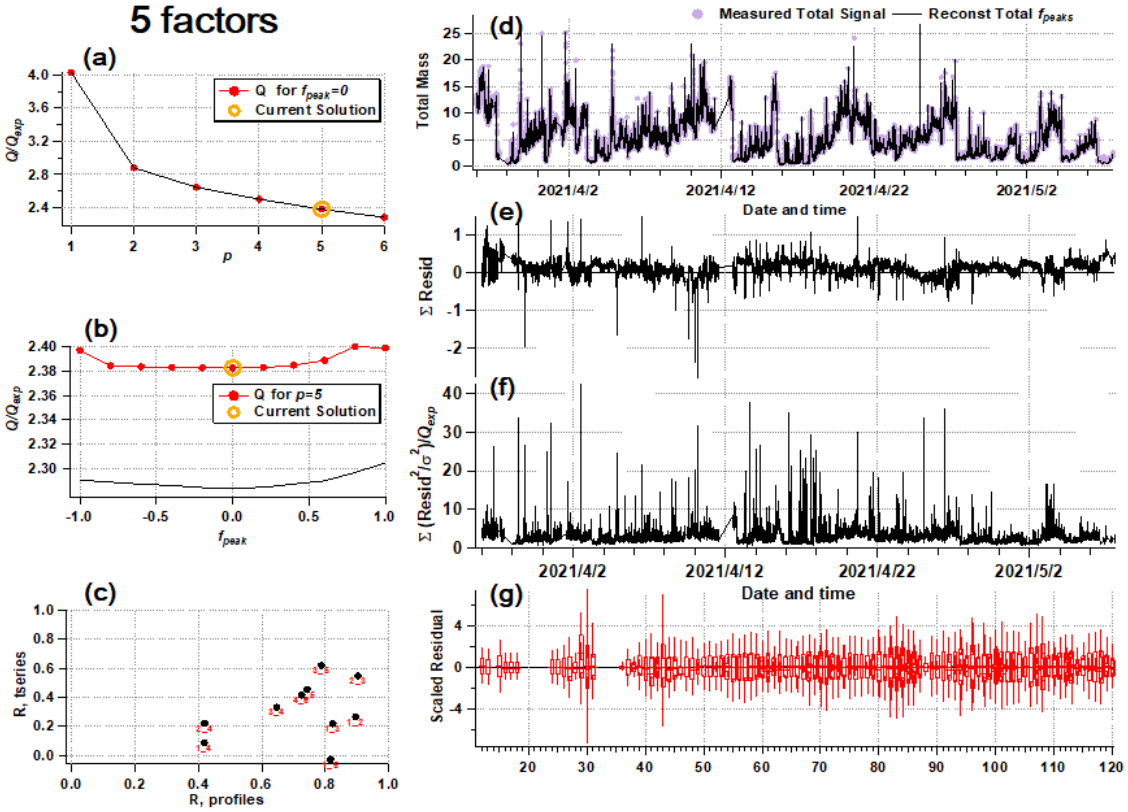

Figure S6.2 Diagnostic plots of the 5 factors of PMF analysis on OA mass spectral matrix for the spring observation.

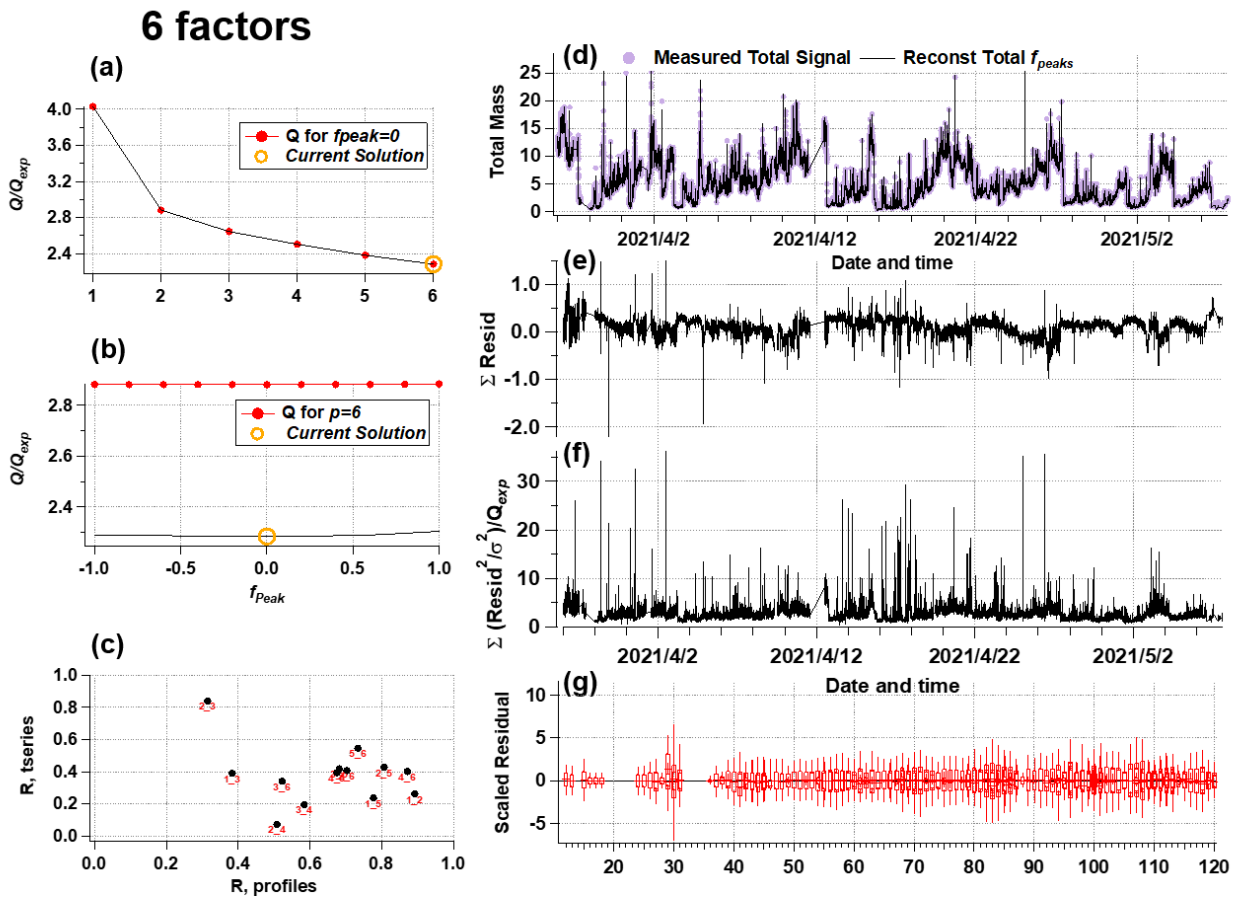

Figure S6.3 Diagnostic plots of the 6 factors of PMF analysis on OA mass spectral matrix for the spring observation.

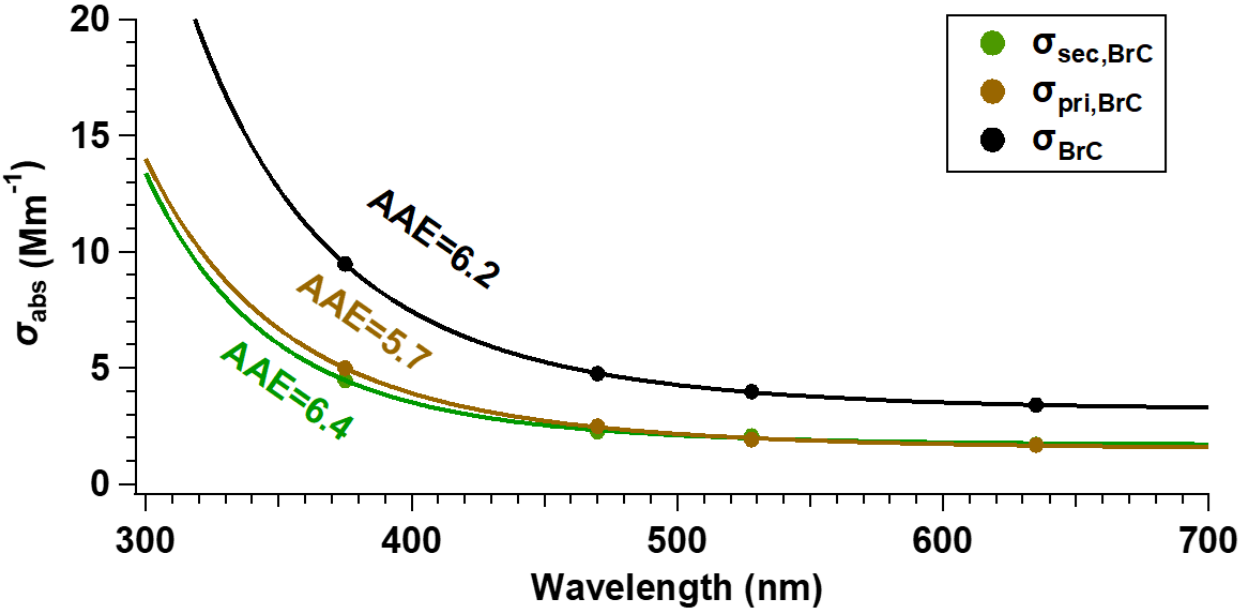

60

61 **Figure S7. Absorption coefficient at λ=375, 470, 528 and 635 nm for total BrC, primary BrC and secondary BrC. The AAE is obtained**
62 **by power fitting on the spectra of absorption coefficient.**

63

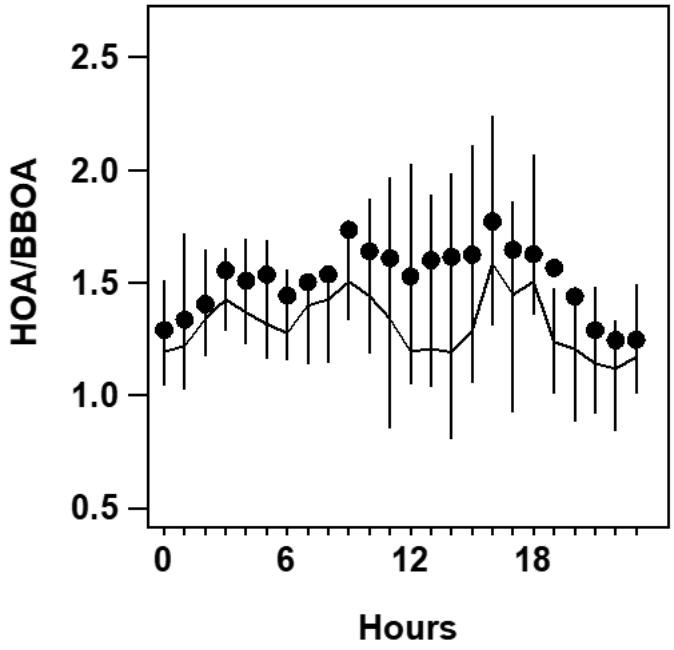

Figure S8. Diurnal variations of HOA/BBOA.

Table S1. Estimated uncertainties of input and output parameters.

Input Parameter	Uncertainty (%)	Output Parameter	Uncertainty (%)
$\left(\frac{\sigma_{abs,total}}{[rBC]}\right)_{pri}$	4[a]	$\sigma_{abs,BrC}$	40
BC mass concentration	20[b]	$\sigma_{abs,priBrC}$	37
MAC	27[c]	$\sigma_{abs,secBrC}$	32
$\sigma_{abs,BC}$	31		
$\sigma_{abs,pri}$	20		
$\sigma_{abs,total}$	25[d-e]		

(a) Wang et al. (2019)
(b) Schwarz et al. (2008)
(c) Taylor et al. (2015)
(d) Duesing et al. (2019)
(e) (Drinovec et al., 2015)

References

Drinovec, L., Močnik, G., Zotter, P., Prévôt, A. S. H., Ruckstuhl, C., Coz, E., Rupakheti, M., Sciare, J., Müller, T., Wiedensohler, A., and Hansen, A. D. A.: The "dual-spot" Aethalometer: an improved measurement of aerosol black carbon with real-time loading compensation, Atmos. Meas. Tech., 8, 1965-1979, 10.5194/amt-8-1965-2015, 2015.

Duesing, S., Wehner, B., Mueller, T., Stoecker, A., and Wiedensohler, A.: The effect of rapid relative humidity changes on fast filter-based aerosol-particle light-absorption measurements: uncertainties and correction schemes, Atmospheric Measurement Techniques, 12, 5879-5895, 10.5194/amt-12-5879-2019, 2019.

Paatero, P. and Tapper, U.: Positive matrix factorization: A non-negative factor model with optimal utilization of error estimates of data values, Environmetrics, 5, 111-126, doi:10.1002/env.3170050203, 1994.

Schwarz, J. P., Spackman, J. R., Fahey, D. W., Gao, R. S., Lohmann, U., Stier, P., Watts, L. A., Thomson, D. S., Lack, D. A., Pfister, L., Mahoney, M. J., Baumgardner, D., Wilson, J. C., and Reeves, J. M.: Coatings and their enhancement of black carbon light absorption in the tropical atmosphere, Journal of Geophysical Research-Atmospheres, 113, 10.1029/2007jd009042, 2008.

Taylor, J. W., Allan, J. D., Liu, D., Flynn, M., Weber, R., Zhang, X., Lefer, B. L., Grossberg, N., Flynn, J., and Coe, H.: Assessment of the sensitivity of core/shell parameters derived using the single-particle soot photometer to density and refractive index, Atmospheric Measurement Techniques, 8, 1701-1718, 10.5194/amt-8-1701-2015, 2015.

Ulbrich, I. M., Canagaratna, M. R., Zhang, Q., Worsnop, D. R., and Jimenez, J. L.: Interpretation of organic components from

Positive Matrix Factorization of aerosol mass spectrometric data, Atmos Chem Phys, 9, 2891-2918, doi:10.5194/acp-9-2891-2009, 2009.

Wang, Q., Han, Y., Ye, J., Liu, S., Pongpiachan, S., Zhang, N., Han, Y., Tian, J., Wu, C., Long, X., Zhang, Q., Zhang, W., Zhao, Z., and Cao, J.: High Contribution of Secondary Brown Carbon to Aerosol Light Absorption in the Southeastern Margin of Tibetan Plateau, Geophysical Research Letters, 46, 4962-4970, 10.1029/2019gl082731, 2019.

Zhang, Q., Jimenez, J., Canagaratna, M., Ulbrich, I., Ng, N., Worsnop, D., and Sun, Y.: Understanding atmospheric organic aerosols via factor analysis of aerosol mass spectrometry: a review, Analytical And Bioanalytical Chemistry, 401, 3045-3067, 10.1007/s00216-011-5355-y, 2011.